Published in final edited form as:
*Toxicol Appl Pharmacol*. 2013 November 1; 272(3): 703–712. doi:10.1016/j.taap.2013.07.023.

# HEMOCOMPATIBILITY AND BIOCOMPATIBILITY OF ANTIBACTERIAL BIOMIMETIC HYBRID FILMS

**M. Carme Coll Ferrer**[1,2], **Uriel N. Eckmann**[1], **Russell J. Composto**[2], and **David M. Eckmann**[1,*]

[1]Department of Anesthesiology and Critical Care, University of Pennsylvania, Philadelphia, PA 19104, USA

[2]Department of Materials Science and Engineering, University of Pennsylvania, Philadelphia, PA 19104, USA

## Abstract

In previous work, we developed novel antibacterial hybrid coatings based on dextran containing dispersed Ag NPs (~5nm, DEX-Ag) aimed to offer dual protection against two of the most common complications associated with implant surgery, infections and rejection of the implant. However, their blood-material interactions are unknown. In this study, we assess the hemocompatibility and biocompatibility of DEX-Ag using fresh blood and two cell lines of the immune system, monocytes (THP-1 cells) and macrophages (PMA-stimulated THP-1 cells). Glass, polyurethane (PU) and bare dextran (DEX) were used as reference surfaces. PU, DEX and DEX-Ag exhibited non-hemolytic properties. Relative to glass (100%), platelet attachment on PU, DEX and DEX-Ag was 15%, 10% and 34%, respectively. Further, we assessed cell morphology and viability, pro-inflammatory cytokines expression (TNF-α and IL-1β), pro-inflammatory eicosanoid expression (Prostaglandin $E_2$, $PGE_2$) and release of reactive oxygen species (ROS, superoxide and $H_2O_2$) following incubation of the cells with the surfaces. The morphology and cell viability of THP-1 cells were not affected by DEX-Ag whereas DEX-Ag minimized spreading of PMA-stimulated THP-1 cells and caused a reduction in cell viability (16% relative to other surfaces). Although DEX-Ag slightly enhanced release of ROS, the expression of pro-inflammatory cytokines remained minimal with similar levels of $PGE_2$, as compared to the other surfaces studied. These results highlight low toxicity of DEX-Ag and hold promise for future applications *in vivo.*

### Keywords

Silver nanoparticles; dextran; hybrid coating; hemocompatibility; cytocompatibility

## Introduction

Current complications associated with implant surgery involve post-operative infections and implant rejection (Sharples et al., 1991). Once the patient develops an infection, the



*Corresponding author: David M. Eckmann, Department of Anesthesiology and Critical Care, University of Pennsylvania, 3400 Spruce St., 6 Dulles-HUP, Philadelphia, PA 19104-4283, Phone: (215) 349-5348, Fax: (215) 349-5078, eckmanndm@uphs.upenn.edu.

microorganisms are extremely resistant to antibiotic therapy and most infections cannot be fully resolved until the biomaterial is removed. The rejection of medical devices is associated with a natural response of the body toward foreign materials. When in contact with blood, foreign materials promote the rapid formation of thrombus that can either adhere to the surface of the material (i.e., a local effect) and disrupt its performance or be detached and carried downstream and eventually occlude a blood vessel (i.e., thromboembolism). These complications aggravate a patient's recovery and result in prolonged hospital stay, need for further medical interventions, increased healthcare cost, and even mortality. Present precautions often require patients to take antibacterial and anticoagulant drugs during for the duration of the implant's use. Hybrid biomimetic films having both antibacterial and antithrombogenic properties are an alternative approach to limiting complications of use and reducing the need for additional therapies.

In previous work, we developed antibacterial biomimetic hybrid films (DEX-Ag) intended for blood contacting devices such as implants and catheters (Ferrer et al., 2012). DEX-Ag coatings were inspired in the endothelial glycocalyx, an irregular brush-like layer that lines the blood vessels and protects them from non-specific interactions. The endothelial glycocalyx is made of a complex blend of polysaccharides and proteins. Within polysaccharides, dextran, known to limit cell and protein adhesion, was the polymer of choice (Massia et al., 2000; Eckmann et al., 2003; Ombelli et al., 2011). The DEX-Ag coatings were prepared by grafting dextran to a substrate embedded with silver nanoparticles (Ag NPs). The methodology involved two steps, the synthesis of Ag NPs *in situ* in the presence of oxidized dextran followed by simultaneous grafting of dextran and the trapping of Ag NPs within the layer. The resulting film displays dextran features as well as individual Ag NPs (5nm) and aggregates, which are embedded within the film. The antibacterial properties of the film were demonstrated against gram positive bacteria, Staphylococcus aureus, the most common microorganism causing surgical site infections (O'Grady et al., 2011). The hybrid films showed reduction in bacteria colonization when compared to control surfaces. Relative to silicon and bare dextran, the hybrid coating strongly reduced bacteria adhesion by 93% and 78%, respectively.

The hemocompatibility and biocompatibility of dextran and derivatives of dextran has been longer known. Clinical uses of dextran (40,000–100,000 Da) include plasma volume expansion and blood flow improvement whereas dextran derivatives are used for instance, as anticoagulant (sulfate ester of dextran) and as oral iron supplementation (iron dextran complex) (Naessens et al., 2005). In contrast, the hemocompatibility and biocompatibility of Ag NPs remains controversial. While several reports focus on the benefits of Ag NPs as a antibacterial, antifungal, anti-viral and anti-inflammatory agent (Zhang and Webster, 2009), others alert of their toxicity (Nair and Laurencin, 2007). *In vitro* exposure of Ag NPs in different cell lines has been associated with disruption of mitochondrial function and increase in reactive oxygen species (ROS) levels, which may lead to cell apoptosis (Braydich-Stolle et al., 2005; Hussain et al., 2005). Although the exact mechanisms by which AgNPs alter mithocondrial function are unknown, Ag NPs react with the thiol groups of proteins and enzymes including key components of the cell's antioxidant defense mechanism such as glutathione, thioredoxin, SOD and thioredoxin peroxidase. As a consequence, Ag NPs may deplete the cell antioxidant defense mechanism which can lead to an accumulation of ROS. Excess of ROS is associated with various human diseases. For instance, ROS play a role in diabetes and neurodegenerative diseases. Furthermore, ROS influences central cellular processes such as proliferation, apoptosis and senescence which are implicated in the development of cancer (Waris and Ahsan, 2006).

The goal of this study was to test whether DEX-Ag elicits specific blood-contact reactions, thrombosis and inflammation, that could limit its potential for in vivo applications. A hard

inorganic surface (glass), a commercially available biomaterial (PU) and dextran (DEX) surfaces were selected as reference surfaces. The hemocompatibility of the surfaces was assessed by hemolysis and thrombogenicity (quantification of platelet adhesion and activation). The biocompatibility of the surfaces was assessed using monocytes and macrophages, cellular components of the immune system that play a critical role in biological responses to materials (Anderson, 2001), e. g., mediate inflammation. Monocytes circulate freely in the body and can maturate into macrophage-like adherent cells to simply replenish macrophages or as a response to inflammation. These two cell types cover three main functions in the body, phagocytosis, antigen presentation and cytokine production. Because of these functions, monocytes and macrophages are commonly used to evaluate biocompatibility of materials. In particular, we used THP-1 cells, a human monocytic cell line, and matured THP-1 cells (macrophage-like) following stimulation with phorbol 12-myrstate 13-acetate (PMA). We assessed their morphological changes and cytotoxicity, monitored the release of three markers of inflammation, TNF-α, IL-1β and $PGE_2$, and examined the release of two ROS, superoxide and hydrogen peroxide, after incubation with the surfaces.

## Materials and methods

### Materials and instruments

All solvents and reagents were of analytical grade and used as received. Dextran from Leuconostoc *ssp.* (Mw = 100 kDa) was purchased from Fluka Chemie (Buchs, Switzerland). 3-aminopropyltriethoxysilane (APTES), sodium periodate ($NaIO_4$), sodium cyanoborohydride ($NaBH_3CN$), silver nitrate ($AgNO_3$), dihydroethidium (DHE), 2′,7′-dichlorodhihydrofluorescein diacetate (DCF-DA) and ethidium homodimer were purchased from Sigma-Aldrich (St. Louis, MI, USA). Square glass slides (25 × 25 $mm^2$), round glass slides (1 cm diameter), phosphate buffered saline ($Ca^{2+}$ and $Mg^{2+}$ free) (PBS), Cyanmethemoglobin Standard and Drabkin's reagent were purchased from Fisher Scientific (Hampton, NH, USA). Tecothane TT-1055D (PU), medical grade aromatic polyether-based thermoplastic polyurethane, was kindly donated by Lubrizol (Wilmington, DE, USA). Calcein, Calcein Violet AM and 7-amino-actinomycin D (7-DAA) were purchased from Invitrogen (Carlsbad, CA, USA). Prior to analyses, the surfaces were sterilized with ethanol.

Epifluorescence microscopy was performed using an Olympus IX70 microscope (Olympus, Melville, NY, USA) outfitted with a Chroma Photofluor metal halide light source (89 North, Burlington, VT, USA). Images were captured using a SensiCam QE camera (The Cooke Corp., Romulus, MI, USA) (2 × 2 binning, 688 × 520). IPLab software was used for image acquisition and to control the LUDL programmable filter wheels, shutters, and focus (Ludl Electronic Products, Hawthorne, NY, USA). ImageJ (NIH, Bethesda, MD, USA) was used for image analysis. Confocal microscopy was performed on an Olympus IX81 with Fluoview FV1000 controller. Fluoview 1.6 was used for image acquisition and ImageJ was used for analysis. Plate reader assays were performed using CHAMELEON™V (Hidex, Turku, Finland). Flow cytometry was performed using BD FACSCalibur and CellQuest software (Becton Dickinson, San Jose, CA, USA). Two-color analysis was performed with FlowJo software (Tree Star Inc., Ashland, OR, USA).

### Cleaning of glass surfaces

The glass slides (round for blood incubation studies and square for all other studies) were cleaned prior further modification using "piranha" solution (70% $H_2SO_4$ and 30% $H_2O_2$) for 20 min at 80 °C, extensively rinsed with deionized water, blown dry with compressed $N_2$ (g) and exposed to ultraviolet light in a UVO-cleaner cleaner (UVO Cleaner model 42, Jelight Co. Inc., Irvine, CA, USA) for 10 min.

### Preparation of DEX and DEX-Ag surfaces

DEX and DEX-Ag surfaces were prepared as previously reported (Ferrer et al., 2012). Briefly, dextran was oxidized using $NaIO_4$ (1:1 molar ratio) at a concentration of 50 mg/mL for 6h, dialyzed for at least 3 days and lyophilized. Ag NPs were synthesized in an aqueous solution of oxidized dextran (2 mL, 1 g/L) using $AgNO_3$ as a precursor agent (1mL, 2 mM) at 70 °C for 30 min. Prior grafting the coatings, surface amination was carried out on glass using the vapor deposition method for 3 h at 70 °C. The aminated surfaces were then submerged in 3 mL of aqueous solution of oxidized dextran (1 mg/mL) or freshly made silver nanoparticles in oxidized dextran containing 75 μL of aqueous solution of $NaBH_3CN$ (100 mg/mL) and were allowed to react in dark conditions overnight. After immobilization, the grafted surfaces were removed from solution, submerged in deionized water for 5 min, rinsed and blown dry with compressed $N_2$ (g).

### Preparation of PU surfaces

PU surfaces were prepared as described somewhere else (Ferrer et al., 2010). Briefly, 250 μL solution of PU (tetrahydrofuran/dichloroethane 1:1, 0.75 wt %) was spun coated (2000 rpm, 15 s) on glass. The coated surfaces were allowed to dry overnight in the hood.

### Blood collection and preparation of platelet rich plasma

Following the UPENN Institutional Review Board protocol, blood was drawn from healthy volunteers by venipuncture into acid citrate (hemolysis assay and blood incubation test) or acid citrate dextrose (platelet adhesion test) as anticoagulant. Platelet-rich plasma (PRP) was isolated from fresh blood by centrifuging at 3500 rpm for 20 min.

### Hemolysis

The hemolysis assay was performed in agreement with standard ASTM F56-08 practice, a colorimetric assay that measures the release of cyanmethemoglobin in solution (ASTM-F756-08, 2000). According to this assay, the hemolytic properties of biomaterials are classified as the percentage of released hemoglobin (% rHb) following blood incubation with the biomaterial at least for 3 h. Non-hemolytic materials are those that experience 0–2% rHb, whereas 2–5% rHb and >5% rHb relates to slightly hemolytic and hemolytic materials, respectively. As a positive and negative control, deionized water and saline (PBS), respectively, were used. 1 mL PBS and 125 μL of diluted blood ([Hb] ~ 10 g/L) were added to all dishes and these were incubated at 37 °C for 3 h on a shaker. Following incubation, the solutions were centrifuged at 700 g for 15 min. The natants were allowed to react at 1:1 volume with Drabkin's reagent (Ricca Chemical, Arlington, TX) for 15 min and their absorbance was measured at 540 nm. The hemolysis ratio was calculated as the supernatant hemoglobin concentration × 100 divided by the total hemoglobin concentration. The hemoglobin concentration in blood was determined by means of a calibration curve.

### Platelet adhesion

PU, DEX and DEX-Ag surfaces were incubated with 0.5 mL of PRP for 1 h at 37 °C under static conditions. As a positive control glass surfaces were used. Following PRP incubation, the surfaces were rinsed with PBS. The adhered platelets were stained using Calcein AM (1.5 μM, 30 min at 37 °C) rinsed and imaged. Calcein-AM is a widely used fluorescent probe that does not interfere with the adhesion process and has proven effective for the assessment of platelet viability with similar reliability as radiolabelling assays (Gibbins and Mahaut-Smith, 2004). For each surface, 5 images were collected using an epifluorescence microscope with 10× objective and viable cells were counted using ImageJ (NIH, Bethesda, MD, USA). The experiment was performed in triplicate.

### Whole blood incubation

The potential of glass, PU, DEX and DEX-Ag to minimize cell activation responses (e.g., neutrophil and platelet activation, neutrophil-platelet interaction, platelet aggregation) was studied by SEM following incubation with fresh drawn whole blood for 1 h at 37 °C on a shaker. As a positive control glass surfaces were used. The adherent platelets were treated for SEM by fixation in 2% gluteraldehyde in cacodylate buffer overnight. Samples were then dehydrated with graded ethanols and dried using HDMS. The experiment was performed in duplicate.

### THP-1 Cell Culture

THP-1 cells and THP-1 cells stably transduced with GFP-actin (Ferrer et al., 2013; Lee et al., 2012) were maintained in suspension culture in RPMI media (Gibco, Grand Island, NY, USA), supplemented with 10% FBS (HyClone, Rockford, IL, USA), 1% penicillin streptomycin (Invitrogen, Carlsbad, CA, USA), and 0.05 mM 2-mercaptoethanol. For all experiments, cells (13,000 cells/$cm^2$) were plated on 35 mm polystyrene petri dishes (BD, Ashland, MA, USA) containing the modified glass slides. THP-1 cells were stimulated with the addition of 1 μg/mL of Phorbol 12-myristate 13-acetate (PMA) for 72 h.

### Morphologic study of THP-1 cells and PMA-stimulated THP-1 cells

The cell morphology of THP-1 cells and PMA-stimulated THP-1 cells after exposure to glass, PU, DEX and DEX-Ag for 3 days was investigated by fluorescence microscopy and confocal microscopy, respectively. The cell surface area contacting the surface of PMA-stimulted THP-1 cells was measured using ImageJ.

### Measurement of non-specific adherence and viability of THP-1 cells

The non-specific adherence of THP-1 cells after exposure to glass, PU, DEX and DEX-Ag surfaces for 1 and 3 days was determined by hydrolysis of an acetoxymetyl ester derivative fluorescent indicator, Calcein Violet AM (750 nM). For each surface, 9 images were collected using 10× objective and viable cells were counted using ImageJ (NIH, Bethesda, MD, USA). This experiment was performed in triplicate. The viability of THP-1 cells after exposure to the surfaces for 3 days was determined by flow cytometry. Following surface exposure, cells were stained with 7-DAA and were transferred into FACs tubes. Mean GFP fluorescence was calculated from 10,000 live cells per sample. Cells that may have clumped together were gated out based on their forward and side scatter profiles.

### Measurement of specific adherence and viability of PMA-stimulated THP-1 cells

The specific adherence of PMA-stimulated THP-1 cells after exposure to glass, PU, DEX and DEX-Ag surfaces for 3 days was determined as described in measurement of non-specific adherence of THP-1 cells. The viability of PMA-stimulated THP-1 cells was determined using Calcein Violet (750 nM) and ethidium homodimer (2 μM).

### Measurement of TNF-α, IL-1β and $PGE_2$ release

THP-1 and PMA-stimulated THP-1 cells were exposed to glass, PU, DEX and DEX-Ag surfaces for 24 h (THP-1 cells only) and 72 h. LPS (10 μg/mL) was used as a positive control. Following incubation, the cell suspensions were pelleted and the supernatant removed and stored in the freezer (−80 °C). The concentrations of TNF-α and IL-1β were measured using a sandwich enzyme-linked immunosorbent assay (ELISA) according to the manufacturer's instructions (Invitrogen, Carlsbad, CA, USA). The concentrations of $PGE_2$ were measured using an ELISA kit (R&D Systems, Inc., Minneapolis, MN, USA). For TNF-α, IL-1β and $PGE_2$, the lowest standard concentrations used were 31 pg/mL, 15.7 pg/mL and 39 pg/mL, respectively.

### Detection of intracellular reactive oxygen species (ROS)

The amount of hydrogen peroxide and superoxide radical was monitored using DCF-DA and DHE stains, respectively. DCF-DA turns fluorescent upon oxidation by the intracellular ROS. DHE, a blue fluorescent probe, emits red fluorescence upon oxidation by superoxide radical. Dead cells were monitored using 7-DAA. Following THP-1 and PMA-stimulated THP-1 cells exposure to glass, PU, DEX and DEX-Ag surfaces for 72 h, the cells were transferred to FACS tubes. PMA-stimulated THP-1 cells were scraped using a cell scraper. Prior analysis, cells were incubated with 5 μM DHE, 20 μM DCF-DA and 5 μL 7-DAA for 5 min at room temperature. Hydrogen peroxide treated cells (0.09%) were used as a positive control for DCF-DA analysis, whereas diethyldithiocarbamic acid (DDC) at a concentration of 200 μM (2 h at 37 °C) was used as a positive control for DHE staining. DCC is a strong inhibitor of superoxide dismutase activity in cells. Cells were analyzed at an excitation wavelength of 488 nm and emission wavelengths of 530 and 610 nm for DCF-DA and DHE, respectively and at excitation wavelength of 546 nm and emission wavelength of 647 nm for 7-DAA. Cells that may have clumped together were gated out based on their forward and side scatter profiles. For each sample 10,000 cells were collected. Dead cell were excluded from the calculations.

### Statistical analysis

Data are presented as mean ± standard deviation. Statistical significance was assessed via Student's t-test (OriginLab, Northampton, MA, USA). Values of $p < 0.05$ were considered statistically significant.

## Results

### Hemolysis

Water (98.6 ± 9.2 % rHb) and saline (0.537 ± 0.005 % rHb) were used as a positive and negative control, respectively. Based on the standard ASTM F56-08 classification, all the PU, DEX and DEX-Ag surfaces studied were non-hemolytic (Table 1). The presence of Ag NPs enhanced the % rHb by two fold relative to PU and DEX while maintaining non-hemolytic properties.

### Platelet adhesion

A significantly lower percentage of platelets adhered to PU, DEX and DEX-Ag as compared to glass (Figure 1A, $p < 0.005$). Relative to glass (100%) the amount of platelets that adhere onto DEX, PU and DEX-Ag was of 15%, 10% and 34%, respectively.

### Blood incubation

All surfaces exhibited platelet adhesion (Figure 1B) while minimizing neutrophil adhesion. However, the platelets response varied within the four surfaces. A common classification of platelet spreading includes five morphological forms describing increasing of activation (Goodman 1998). These are discoid or round, dendritic or early pseudopodial, spread dendritic, spreading and fully spread. According to this classification, platelets in contact with DEX, DEX-Ag and glass reached fully spread and spreading morphologies. These, in turn, formed a based layer for large number of pseudopodial platelets on top on glass and at lower extent on dextran. Platelets on PU were evenly distributed over the surface and were almost entirely dendritic and spread-dendritic morphologies.

### Effect on cell morphology

Independent of the surface studied, THP-1 cells remained round in shape (data not shown). Upon PMA-stimulation, changes in cell morphology with the different surfaces were

observed. Figure 2 shows representative 2D- and 3D-morphology images of PMA-stimulated THP-1 cells after 3 days exposure to glass, PU, DEX and DEX-Ag surfaces. The cells spread the most on glass (Figure 2A), where the majority of cells exhibited amoeboid morphology and some exhibited round morphology. On PU (Figure 2B), the cells spread moderately leading to all type of shapes, elongated, amoeboid and round shape cells. In contrast, DEX and DEX-Ag surfaces (Figure 2C and 2D, respectively) showed the least spread cells with the majority of cells exhibiting round morphology and some showed elongated morphology. To further quantify these observations, the surface area of at least 70 cells per surface was measured and compared. Gaussian fits for each surface have been included in Figure 2. In particular, PMA-stimulated cells adhered on glass, PU, DEX and DEX-Ag exhibited average surface area of 539 ± 29, 492 ± 36, 439 ± 24 and 420 ± 24 $\mu m^2$, respectively.

## Cell adherence and viability

Within THP-1 cells, most cells circulated freely in the blood stream (Figure 3A). After 1 day (grated bars), glass showed the highest number of adhered cells, i.e., activated non-specifically, followed by PU. Some THP-1 cells also adhered on DEX but at significantly lesser extent. In particular, DEX-Ag, the surface with the least adhered THP-1 cells, showed a reduction of cells adhered of 90% and 94% relative to PU and glass, respectively ($p < 0.005$). After 3 days incubation the overall number of adhered THP-1 cells increased (solid bars). The highest number of adhered cells was also observed on glass, but followed by DEX and PU. Similar to 1 day incubation, DEX-Ag showed the least number of adhered cells after 3 days incubation. By comparing the number of adhered THP-1 cells between 1 and 3 days incubation for the different surfaces, cells adhered increased after 3 day incubation by a factor of 4 for glass and PU and by a factor of 23 and 19 for DEX and DEX-Ag, respectively relative to 1 day incubation. Although DEX-Ag showed a significant increase of adhered THP-1 cells after 3 days, DEX-Ag still showed a reduction of 55% and 70% relative to PU and glass, respectively ($p < 0.005$). THP-1 cells that adhered remained mainly round on all surfaces but appeared slightly larger (less than 1 fold) on glass after 3 days incubation. Independent of the number of THP-1 cells adhered non-specifically on the surfaces, all surfaces showed analogous cell viability (~95%, Figure 3B).

Upon PMA stimulation of THP-1 cells, cells adhered to the surfaces in a similar fashion as non-stimulated THP-1 cells after incubation for 3 days (Figure 3C). Cells adhered on glass the most, followed by DEX and PU. DEX-Ag exhibited the least number of adhered cells, a reduction of 31% and 51% relative to PU and glass, respectively. In terms of cell viability (Figure 3D), glass, PU and DEX exhibited similar viability (~ 95%) whereas a 16% decrease on cell viability was observed on DEX-Ag ($p < 0.005$).

## TNF-α and IL-1β release

Independent of which of the cytokine (TNF- α, IL-1β) and which of the surface of study (glass, PU, DEX and DEX-Ag) were used, THP-1 cells did not elicit detectable cytokine levels, e. g., levels measured were lower than lowest standard point. In contrast, LPS-treated THP-1 cells released significant amounts of TNF-α (850 ± 40 pg/mL) and IL-1β (1334 ± 65 pg/mL), respectively.

Upon PMA-stimulation, THP-1 cells released higher amounts of TNF-α (Figure 4A) and IL-1β (Figure 4B). The lowest amount of TNF-α was detected on DEX-Ag, followed by PU whereas significant larger amount of TNF-α was detected on DEX, a 5–fold increase as compared to glass. As expected, the largest amount of TNF-α was detected in LPS-treated PMA-stimulated THP-1 cells (1634 ± 78 pg/mL). Similarly, cells incubated on DEX presented high release of IL-1β ($p < 0.005$) whereas cells on DEX-Ag exhibited the lowest.

DEX-Ag decreased IL-1β release of PMA-stimulated THP-1 cells by 90%, 85% and 96% relative to glass, PU and DEX ($p < 0.005$). Although PMA-stimulated THP-1 cells on DEX exhibited significant amount of IL-1β as compared to the other surfaces studied, the IL-1β released was only about one-fourth of the amount released by LPS-treated PMA-stimulated THP-1 cells (3048 ± 399 pg/mL).

### Release of $PGE_2$

PMA-stimulated THP-1 cells elicited greater amounts of $PGE_2$ (Figure 5B) as compared to non-stimulated THP-1 cells (Figure 5A). Within cell type, cells released comparable amount of $PGE_2$ independently of the surface of study. In particular, THP-1 cells released ~60 pg $PGE_2$/mL whereas PMA-stimulated THP-1 cells released ~ 250 pg $PGE_2$/mL. LPS-treated cells exhibited a significant amount of $PGE_2$ as compared to the other surfaces studied (211 ± 67 pg/mL and 491 ± 28 pg/mL were released by THP-1 and PMA-stimulated THP-1 cells, respectively.)

### Release of ROS

In general, PMA stimulation of THP-1 cells minimized the number of cells that release hydrogen peroxide as compared to non-stimulated THP-1 cells for all the surfaces studied (over 5 fold decrease) as well as its intensity per cell on PU and DEX-Ag (by 2 and 5 fold decrease, respectively). However, the fluorescence intensity representing hydrogen peroxide per cell was observed to increase upon PMA-stimulation of THP-1 cells on DEX (3 fold).

In contrast, the amount of cells expressing superoxide was within the same range independently of PMA-stimulation (5–7% cell population). DEX-Ag exhibited the largest percentage of cells expressing superoxide prior to PMA-stimulation (6.7% vs 5.5% and 5.1%, for PU and DEX, respectively) but intermediate upon PMA-stimulation (6.4% vs 6.7% and 6.1% for PU and DEX, respectively) with similar fluorescence intensity. Although THP-1 cells on DEX exhibited the greatest superoxide levels per cell independent of PMA-stimulation, these were within less than 2 fold those of PU and DEX-Ag.

## Discussion

New biocoatings intended for blood contacting devices would benefit from possessing antibacterial properties while remaining biocompatible to minimize the commonly encountered infection and implant rejection complications associated with implant surgery. Our approach to prepare hybrid biocoatings involves dextran, an α(1–6)-linked glycan, water soluble and neutral, with multiple reactive sites available for subsequent functionalization. Importantly, dextran has demonstrated outstanding properties against nonspecific protein adhesion by our group (Ombelli et al., 2005; Ferrer et al., 2010) and others (Piehler et al., 1999; Frazier et al., 2000; Martwiset et al., 2006). Although the hemocompatibility and biocompatibility of dextran has been known longer, it is necessary to ensure that these properties are retained when embedding Ag NPs in dextran. In the present study we used blood and a human monocytic part of the immune system and commonly used to interrogate the biocompatibility of materials, THP-1 and PMA-stimulated THP-1 cells, to study the hemocompatibility and biocompatibility of DEX-Ag. As controls, we also studied a hard inorganic material (glass), a biocompatible commercial polymer (PU) and bare dextran.

Ag NPs have shown to induce hemolysis and although, the mechanism by which Ag NPs induce hemolysis is not well understood, in contact with body fluids, metallic silver ionizes and releases Ag+ as a function of the particle surface area. Silver ions can enhance suicidal red blood cell (RBC) death due to decreased ATP content and phosphatidylserine exposure

to the surface (Sopjani et al., 2009). Further, silver ions can quickly react with anionic ligands (e.g., chloride, thiols) which can damage proteins and antioxidants (Johnston et al., 2010). In general, greater levels of *in vitro* hemolysis have been related to greater surface area, increased silver ion release, and direct interaction with RBCs of nanosized Ag over micro-sized particles (Choi et al., 2011). Our hybrid coatings, prepared with Ag NPs (5 nm) embedded in dextran, exhibited non-hemolytic properties. This finding suggests slow release of Ag+ due to low Ag NPs content and stabilization of Ag NPs in dextran. In previous work, we measured a loss of 20 wt% of Ag of an initial 7 wt % during bacterial experiments (6 h incubation at 37 °C, and 100 rpm) as determined by Rutherford Backscattering technique (Ferrer et al., 2012).

Following material-blood interaction, thrombus formation, i.e., platelet aggregation, is the earliest and most common consequence, which is initiated with platelet adhesion and activation. Although the accountability of Ag NPs towards thrombus formation has been researched, remains controversial. For instance, Shrivastava et al. (2009), demonstrated the antiplatelet activity of Ag NPs *in vivo* and *in vitro* whereas Stevens et al. (2009) observed that Ag NPs on coated catheters enhanced thrombin formation and platelet activation while reducing platelet adhesion. In our studies, DEX-Ag coatings minimized platelet adhesion (66% reduction) relative to glass. This is a significant finding considering that glass has shown significant lower platelet adhesion than other biocompatible polymers, such as PVC and polyethylene (Mohammad et al., 1974). Moreover, DEX-Ag exhibited a spreading/fully spread monolayer of platelets, which have been shown important for clinical biocompatibility of a biomaterial (Goodman, 1999).

To evaluate the biocompatibility of the hybrid coatings, we evaluated the THP-1 cells and PMA-stimulated THP-1 cells following incubation with the surfaces. In particular, we assessed cell morphology, cell viability, cellular release of three pro-inflammatory markers (TNF-α, IL-1β, $PGE_2$) and cellular release of ROS.

The hybrid coatings and other surfaces studied did not trigger THP-1 cell activation (e.g., adherence), alter cell morphology or diminish cell viability. Upon PMA stimulation, THP-1 cells adhered onto surfaces. As others, we observed dependence of cell morphology on surface. The resulting cell morphology has been related to the chemistry, topography, modulus and more recently, to the biocompatibility of the surface. In particular, hydrophilic, lower modulus and biocompatible surfaces have been shown to minimize THP-1 cell attachment and activation (i.e., less cell spreading) (Irwin et al., 2008; Ferraz et al., 2010; Lee et al., 2012). Our studies showed fewer adhered cells on DEX-Ag relative to the other surfaces studied. Whereas a reduction of adhered cells have been associated to biocompatibility by others (Lee et al., 2012), we observed a 16% reduction in cell viability on DEX-Ag. This reduction in cell viability may explain increased hemolysis ratio measured on DEX-Ag relative to the other surfaces, while still maintaining non-hemolytic properties. The toxicity of Ag NPs (20 nm and 40 nm) towards PMA-stimulated THP-1 cells has been reported by Haase et al. ( 2011). Their studies showed a marked reduction in cell viability with Ag NPs concentration and exposure time (24 h and 48 h). For instance, they reported that incubation of the cells with Ag NPs (20 nm, 50 μg/mL) for 24 h and 48 h resulted in about 40% and 20% cell viability, respectively. Compared to their results, the DEX-Ag toxicity toward PMA-stimulated THP-1 cells which was measured after 72 h incubation with the cells is minimal (77% vs 95% of other surfaces studied). Further, the cell morphology was found dependent on the surface, but not on the presence of Ag NPs. Cells spread the most on glass, followed by PU. The least spread cells were observed on DEX and DEX-Ag. These observations are in agreement with previous studies of PMA-stimulated THP-1 cells incubated on glass, PU and DEX reported in the literature (Tsai et al., 2011a; Lee et al., 2012) and correlate well with modulus of the surfaces (Irwin et al., 2008). Glass,

the stiffest surface studied, resulted in spread PMA-stimulated THP-1 cells whereas the softest hydrophilic surfaces, DEX and DEX-Ag exhibit round cell morphologies.

One of the first responses of the immune system to infection is inflammation. Two of the pro-inflammatory cytokines studied, TNF-α and IL-1β, are secreted via different pathways by monocytes and activated macrophages in response to inflammation and contact stimulation (e.g., foreign surface). These cytokines are important immunoregulatory molecules. However, when produced in large quantities they can trigger (mediate and amplify) a large inflammatory response which has been associated with several diseases (e.g., Alzheimer's disease). During inflammatory responses, cytokines and other unknown signals activate TNF-α. Once activated, it can induce excessive cell proliferation that can lead to cancer. In addition, it can activate the transcription factors of nuclear factor-kappaB (NF-kB) pathway, which further enhances the progression and proliferation of cells to tumors by suppressing cell death induced by c-Jun-N-terminal kinase (JNK) (Papa et al., 2004). These pathways have been shown to mediate LPS-induced adhesion and correlate with the high levels of pro-inflammatory cytokines observed in THP-1 and PMA-stimulated THP-1 cells in response to LPS. In contrast, DEX-Ag and PU exhibited minimal release of cytokines, as compared to glass and DEX. High dextran concentrations are known to induce TNF-α and IL-1β. For instance, dextran sulfate solutions are used to induce colitis in mice (Cooper et al., 1993). In agreement with previous studies (Schwende et al., 1996), we observed greater release of TNF-α and IL-1β upon PMA stimulation of THP-1 cells. By comparing DEX-Ag with DEX, our findings stressed the role of Ag NPs in minimizing inflammatory responses. These results contrast with those of Trickler et al. (2010) who demonstrated that Ag NPs (25 nm) enhance TNF-α and IL-1β in a time-dependent manner in primary rat brain microvessel endothelial cells. However, their studies were limited to a maximum of 8 h incubation-time, whereas our studies incorporate 3 days of incubation with the surfaces and a different cell line. Importantly, the anti-inflammatory effects of Ag NPs have been demonstrated *in vivo* by other groups (Wong and Liu, 2010). Nadworny et al. (2008) explored the effect of AgNPs using a porcine model of contact dermatitis, while Bhol and Schechter (2007) utilized AgNPs in a rat model of ulcerative colitis. Both studies concluded that Ag NPs had direct anti-inflammatory effects (based on TNF-α and IL-1β measurements) and improved the healing process significantly compared to controls.

Other mediators of inflammation are eicosanoids, a group of biologically active oxygenated unsaturated fatty acids derived from arachidonic acid by the action of cyclooxygenases, lipoxygenases, and cytochrome P450 mono-oxygenases. Eicosanoids have been shown to play a role in inflammation and have been also recently linked to carcinogenesis (Greene et al., 2011). The eicosanoid family includes prostaglandins such as $PGE_2$, the most common prostaglandin found in different human cancers including colon, lung, breast, and head and neck cancers. $PGE_2$ is also known to suppress the immune responses by inhibiting macrophages, T cells and natural killer activity resulting in pro-tumorigenic activity. Whereas increased pro-inflammatory cytokines are required for tumor invasion and growth, several studies have shown that $PGE_2$ suppresses TNF-α in THP-1 cells (Weigent et al., 1990; Choi et al., 1996). To verify that the low levels of cytokines released by DEX-Ag lead to a true reduced inflammatory potential, we also evaluated the release of $PGE_2$ following incubation with the surfaces for 3 days. In agreement with previous studies (Perezperez et al., 1995), we observed greater release of $PGE_2$ upon PMA-stimulation of THP-1 cells. Independent of cell type, all surfaces released comparable amount of $PGE_2$, confirming the anti-inflammatory behavior of DEX-Ag surfaces.

NP-induced toxicity has been associated with ROS enhancement (Nishanth et al., 2011). ROS in cells are traditionally generated for the purpose of killing invading microorganisms. However, they can also cause damage to nearby tissues, and are thought to be of pathogenic

significance in a large number of diseases (Babior, 2000). Within NPs, AgNPs have been linked with enhancement of ROS generation in several cell lines as a function of dose, exposure, particle size and matrix (Kim and Ryu, 2012). For instance, a 10× fold increase in ROS levels was observed in alveolar macrophages after 24 h incubation with 50 μg/mL Ag NPs (15 nm) (Carlson et al., 2008) and a drastic increase in ROS levels was detected in THP-1 cells following 6–24 h incubation with PVP-coated Ag NPs (70 nm) (Foldbjerg et al., 2009). In contrast, our hybrid coatings did not particularly alter ROS levels as compared to PU and DEX. Few studies have appeared regarding the effect of ROS in THP-1 cells. Haugen et al. (1999) studied the effect of PMA-stimulation of THP-1 cells on oxidants. Although they observed that PMA-stimulation of THP-1 cells induced a rapidly increase in superoxide radical (within 1 h incubation), they detected similar levels of superoxide and hydrogen in THP-1 cells independently of PMA-stimulation after 24 h incubation. Other groups have reported an enhancement of superoxide levels and phagocytic activity upon PMA-stimulation (with up to 24 h incubation time). A longer incubation time study indicated a reduction in the capacity to produce hydrogen peroxide and superoxide radical upon PMA-stimulation after 4 days incubation time with larger levels of hydrogen peroxide over superoxide radical (Nakagawara et al., 1981). The latter is in agreement with the data presented herein. These higher levels of hydrogen peroxide observed after several incubation days may be due to the action of superoxide dismutase that destroys the free radical superoxide by converting it to hydrogen peroxide (Droge, 2002). However, because the cellular production of ROS is very sensitive towards environment, differences in experimental setup may impact the release of ROS and therefore, comparison between different studies available in the literature is not easily performed or interpreted.

In this work, we have assessed DEX-Ag for two of the first major biological responses that typically occur following implant of a biomaterial (Anderson et al., 2008), blood-material interactions (hemolysis, thrombosis) and inflammation (monocytes and macrophages). Overall, DEX-Ag coatings showed low toxicity and minimal inflammatory potential, thus, making them promising for *in vivo* applications. In particular, DEX-Ag coatings may be advantageous to minimize the rate of surgical-site infections (SSIs), the second most common type of healthcare associated infection (HAI) in U.S. hospitals (290,000 per year) accounting for the greatest additional healthcare cost, between $3.5 and 10 billion per year (CDPH, 2011). Having high versatility, these hybrid coatings can be used to enhance the biocompatibility of other materials, such as PU (Tsai et al., 2011b) and titanium (Shi et al., 2009), by various graft-linking reactions.

## Conclusions

We have studied the interaction of DEX-Ag with blood, monocytes (THP-1 cells) and macrophages (PMA-stimulated THP-1 cells) and demonstrated that our hybrid coatings are non-hemolytic, exhibited low platelet adhesion, minimal inflammatory potential and ROS release. Further, the hybrid coatings were biocompatible towards monocytes but decreased the cell viability of macrophages by 16%. Overall, DEX-Ag coatings showed low toxicity and minimal inflammatory potential, thus, making them promising for in vivo applications.

## Acknowledgments

We acknowledge the support of NIH Grants R01 HL060230 and T32 HL007954 and NSF Grants NSEC DMR08-32802 and DMR09-07493. MCCF thanks Dr. Stanley Stachelek (The Children's Hospital of Philadelphia) for providing GFP-actin transduced THP-1 cells, Ivan J. Dmochowski for access to confocal microscope, Nancy Tomczik for ELISA assay training, Dr. Tatyana Milanova for performing flow cytometry and Dr. Sekar Nagasami for SEM training.

## References


Anderson JM. Biological responses to materials. Annu Rev Mater Res. 2001; 31:81–110.

Anderson JM, Rodriguez A, Chang DT. Foreign body reaction to biomaterials. Semin Immunol. 2008; 20:86–100. [PubMed: 18162407]

ASTM-F756-08. Standard practice for assessment of hemolytic properties of materials. 2000.

Babior BM. Phagocytes and oxidative stress. Am J Med. 2000; 109:33–44. [PubMed: 10936476]

Bhol KC, Schechter PJ. Effects of nanocrystalline silver (NPI 32101) in a rat model of ulcerative colitis. Digest Dis Sci. 2007; 52:2732–2742. [PubMed: 17436088]

Braydich-Stolle L, Hussain S, Schlager JJ, Hofmann MC. In vitro cytotoxicity of nanoparticles in mammalian germline stem cells. Toxicol Sci. 2005; 88:412–419. [PubMed: 16014736]

Carlson C, Hussain SM, Schrand AM, Braydich-Stolle LK, Hess KL, Jones RL, Schlager JJ. Unique cellular interaction of silver nanoparticles: size-dependent generation of reactive oxygen species. J Phys Chem B. 2008; 112:13608–13619. [PubMed: 18831567]

CDPH. Key findings and public health actions. California department of health; 2011.

Choi J, Reipa V, Hitchins VM, Goering PL, Malinauskas RA. Physicochemical characterization and in vitro hemolysis evaluation of silver nanoparticles. Toxicol Sci. 2011; 123:133–143. [PubMed: 21652737]

Choi SS, Gatanaga M, Granger GA, Gatanaga T. Prostaglandin-E(2) regulation of tumor necrosis factor receptor release in human monocytic THP-1 cells. Cell Immunol. 1996; 170:178–184. [PubMed: 8660816]

Cooper HS, Murthy SNS, Shah RS, Sedergran DJ. Clinicopathological study of dextran sulfate sodium experimental murine colitis. Lab Invest. 1993; 69:238–249. [PubMed: 8350599]

Droge W. Free radicals in the physiological control of cell function. Physiol Rev. 2002; 82:47–95. [PubMed: 11773609]

Eckmann DM, Tsai IY, Tomczyk N, Weisel JW, Composto RJ. Hyaluronan and dextran modified tubes resist cellular activation with blood contact. Colloids Surf B Biointerfaces. 2003; 108:44–51. [PubMed: 23524078]

Ferraz N, Hong J, Santin M, Karlsson Ott M. Nanoporosity of alumina surfaces induces different patterns of activation in adhering monocytes/macrophages. Int J Biomater. 2010; 2010:402715–402715. [PubMed: 21234322]

Ferrer MCC, Hickok NJ, Eckmann DM, Composto RJ. Antibacterial biomimetic hybrid films. Soft Matter. 2012; 8:2423–2431. [PubMed: 23807896]

Ferrer MCC, Sobolewski P, Composto RJ, Eckmann DM. Cellular uptake and intracellular cargo release from dextran based nanogel drug carriers. J Nanotechnol Eng Med. 2013; 4:1–8.

Ferrer MCC, Yang S, Eckmann DM, Composto RJ. Creating biomimetic polymeric surfaces by photochemical attachment and patterning of dextran. Langmuir. 2010; 26:14126–14134. [PubMed: 20712352]

Foldbjerg R, Olesen P, Hougaard M, Dang DA, Hoffmann HJ, Autrup H. PVP-coated silver nanoparticles and silver ions induce reactive oxygen species, apoptosis and necrosis in THP-1 monocytes. Toxicol Lett. 2009; 190:156–162. [PubMed: 19607894]

Frazier RA, Matthijs G, Davies MC, Roberts CJ, Schacht E, Tendler SJB. Characterization of protein-resistant dextran monolayers. Biomaterials. 2000; 21:957–966. [PubMed: 10735473]

Gibbins, JM.; Mahaut-Smith, MP. Platelets and Megakaryocytes. In: Gibbins, JM.; Mahaut-Smith, MP., editors. Methods in Molecular Biology. Humana Press; New York: 2004.

Goodman SL. Sheep, pig, and human platelet-material interactions with model cardiovascular biomaterials. J Biomed Mater Res. 1999; 45:240–250. [PubMed: 10397982]

Greene ER, Huang S, Serhan CN, Panigrahy D. Regulation of inflammation in cancer by eicosanoids. Prostaglandins & Other Lipid Mediat. 2011; 96:27–36.

Haase A, Tentschert J, Jungnickel H, Graf P, Mantion A, Draude F, Plendl J, Goetz ME, Galla S, Mašić A, Thuenemann AF, Taubert A, Arlinghaus HF, Luch A. Toxicity of silver nanoparticles in human macrophages: uptake, intracellular distribution and cellular responses. J Phys: Conf Ser. 2011; 304:012030.

Haugen TS, Skjonsberg OH, Kahler H, Lyberg T. Production of oxidants in alveolar macrophages and blood leukocytes. Eur Respir J. 1999; 14:1100–1105. [PubMed: 10596697]

Hussain SM, Hess KL, Gearhart JM, Geiss KT, Schlager JJ. In vitro toxicity of nanoparticles in BRL 3A rat liver cells. Toxicol in Vitro. 2005; 19:975–983. [PubMed: 16125895]

Irwin EF, Saha K, Rosenbluth M, Gamble LJ, Castner DG, Healy KE. Modulus-dependent macrophage adhesion and behavior. J Biomat Sci Polym Ed. 2008; 19:1363–1382.

Johnston HJ, Hutchison G, Christensen FM, Peters S, Hankin S, Stone V. A review of the in vivo and in vitro toxicity of silver and gold particulates: Particle attributes and biological mechanisms responsible for the observed toxicity. Crit Rev in Toxicol. 2010; 40:328–346. [PubMed: 20128631]

Kim S, Ryu DY. Silver nanoparticle-induced oxidative stress, genotoxicity and apoptosis in cultured cells and animal tissues. J Appl Toxicol. 2012; 33:78–89. [PubMed: 22936301]

Lee HS, Stachelek SJ, Tomczyk N, Finley MJ, Composto RJ, Eckmann DM. Correlating macrophage morphology and cytokine production resulting from biomaterial contact. J Biomed Mater Res A. 2012; 101:203–212. [PubMed: 22847892]

Martwiset S, Koh AE, Chen W. Nonfouling characteristics of dextran-containing surfaces. Langmuir. 2006; 22:8192–8196. [PubMed: 16952261]

Massia SP, Stark J, Letbetter DS. Surface-immobilized dextran limits cell adhesion and spreading. Biomaterials. 2000; 21:2253–2261. [PubMed: 11026631]

Mohammad SF, Hardison MD, Glenn CH, Morton BD, Bolan JC, Mason RG. Adhesion of human-blood platelets to glass and polymer surfaces. 1 studies with platelets in plasma. Haemostasis. 1974; 3:257–270. [PubMed: 4219776]

Nadworny PL, Wang J, Tredget EE, Burrell RE. Anti-inflammatory activity of nanocrystalline silver in a porcine contact dermatitis model. Nanomedicine. 2008; 4:241–251. [PubMed: 18550449]

Naessens M, Cerdobbel A, Soetaert W, Vandamme EJ. Leuconostoc dextransucrase and dextran: production, properties and applications. J Chem Technol Biotechnol. 2005; 80:845–860.

Nair LS, Laurencin CT. Silver nanoparticles: synthesis and therapeutic applications. J Biomed Nanotechnol. 2007; 3:301–316.

Nakagawara A, Nathan CF, Cohn ZA. Hydrogen peroxide metabolism in human monocytes during differentiation in vitro. J Clin Invest. 1981; 68:1243–1252. [PubMed: 6271809]

Nishanth RP, Jyotsna RG, Schlager JJ, Hussain SM, Reddanna P. Inflammatory responses of RAW 264.7 macrophages upon exposure to nanoparticles: Role of ROS-NF kappa B signaling pathway. Nanotoxicology. 2011; 5:502–516. [PubMed: 21417802]

O'Grady, NP.; Alexander, MA.; Burns, LA.; Dellinger, P.; Garland, J.; Heard, SO.; Lipsett, PA.; Masur, H.; Mermel, LA.; Pearson, ML.; Raad, II.; Randolph, A.; Rupp, ME.; Saint, S. Healthcare Infection Control Practices Advisory Committee. Guidelines for the prevention of intravascular catheter-related infections. Health and Human Services; USA: 2011.

Ombelli M, Composto RJ, Meng QC, Eckmann DM. A quantitative and selective chromatography method for determining coverages of multiple proteins on surfaces. J Chromatog B Analyt Technol Biomed Life Sci. 2005; 826:198–205.

Ombelli M, Costello L, Postle C, Anantharaman V, Meng QC, Composto RJ, Eckmann DM. Competitive protein adsorption on polysaccharide and hyaluronate modified surfaces. Biofouling. 2011; 27:505–518. [PubMed: 21623481]

Papa S, Zazzeroni F, Pham CG, Bubici C, Franzoso G. Linking JNK signaling to NF-kappa B: a key to survival. J Cell Sci. 2004; 117:5197–5208. [PubMed: 15483317]

Perezperez GI, Shepherd VL, Morrow JD, Blaser MJ. Activation of human thp-1 cells and rat bone-marrow-derived macrophages by helicobacter-pylori lipopolysaccharide. Infect Immun. 1995; 63:1183–1187. [PubMed: 7890370]

Piehler J, Brecht A, Hehl K, Gauglitz G. Protein interactions in covalently attached dextran layers. Colloids Surf B Biointerfaces. 1999; 13:325–336.

Schwende H, Fitzke E, Ambs P, Dieter P. Differences in the state of differentiation of THP-1 cells induced by phorbol ester and 1,25-dihydroxyvitamin D-3. J Leukocyte Biol. 1996; 59:555–561. [PubMed: 8613704]

Sharples LD, Caine N, Mullins P, Scott JP, Solis E, English TAH, Large SR, Schofield PM, Wallwork J. Risk factor-analysis for the major hazards following heart-transplantation - rejection, infection, and coronary occlusive disease. Transplantation. 1991; 52:244–252. [PubMed: 1871797]

Shi Z, Neoh KG, Kang ET, Poh C, Wang W. Titanium with surface-grafted dextran and immobilized bone morphogenetic protein-2 for inhibition of bacterial adhesion and enhancement of osteoblast functions. Tissue Eng Part A. 2009; 15:417–426. [PubMed: 18837650]

Shrivastava S, Bera T, Singh SK, Singh G, Ramachandrarao P, Dash D. Characterization of antiplatelet properties of silver nanopartides. Acs Nano. 2009; 3:1357–1364. [PubMed: 19545167]

Sopjani M, Foeller M, Haendeler J, Goetz F, Lang F. Silver ion-induced suicidal erythrocyte death. J Appl Toxicol. 2009; 29:531–536. [PubMed: 19444854]

Stevens KNJ, Crespo-Biel O, van den Bosch EEM, Dias AA, Knetsch MLW, Aldenhoff YBJ, van der Veen FH, Maessen JG, Stobberingh EE, Koole LH. The relationship between the antimicrobial effect of catheter coatings containing silver nanoparticles and the coagulation of contacting blood. Biomaterials. 2009; 30:3682–3690. [PubMed: 19394689]

Trickler WJ, Lantz SM, Murdock RC, Schrand AM, Robinson BL, Newport GD, Schlager JJ, Oldenburg SJ, Paule MG, Slikker W Jr, Hussain SM, Ali SF. Silver nanoparticle induced blood-brain barrier inflammation and increased permeability in primary rat brain microvessel endothelial cells. Toxicol Sci. 2010; 118:160–170. [PubMed: 20713472]

Tsai IY, Kuo CC, Tomczyk N, Stachelek SJ, Composto RJ, Eckmann DM. Human macrophage adhesion on polysaccharide patterned surfaces. Soft Matter. 2011a; 7:3599–3606. [PubMed: 21479122]

Tsai IY, Tomczyk N, Eckmann JI, Composto RJ, Eckmann DM. Human plasma protein adsorption onto dextranized surfaces: A two-dimensional electrophoresis and mass spectrometry study. Colloids and Surf B Biointerfaces. 2011b; 84:241–252.

Waris G, Ahsan H. Reactive oxygen species: role in the development of cancer and various chronic conditions. J of Carcinog. 2006; 5:14–14. [PubMed: 16689993]

Weigent DA, Carr DJJ, Blalock JE. Bidirectional communication between the neuroendocrine and immune-systems - common hormones and hormone receptors. Ann N Y Acad Sci. 1990; 579:17–27. [PubMed: 2186684]

Wong KKY, Liu X. Silver nanoparticles-the real "silver bullet" in clinical medicine? Medchemcomm. 2010; 1:125–131.

Zhang L, Webster TJ. Nanotechnology and nanomaterials: Promises for improved tissue regeneration. Nano Today. 2009; 4:66–80.

## Highlights

- We examined specific blood-contact reactions of dextran doped with Ag NPs coatings
- Biocompatibility was assessed with THP-1 cells and PMA-stimulated THP-1 cells
- Glass, polyurethane and dextran were used as reference surfaces
- Hybrid coatings exhibited non-hemolytic properties
- Low toxicity, inflammatory potential and ROS make them promising for *in vivo* applications

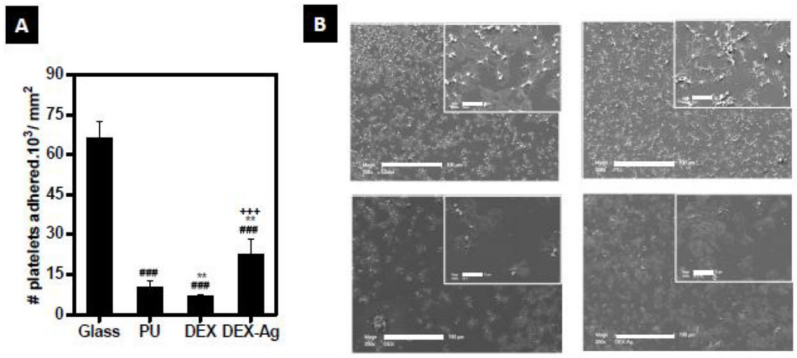


**Figure 1.**

Hemocompatibility studies. (a) Number of platelets adhered after 1h incubation of PRP. Statistical significance: ### $p<0.005$ versus glass, ** $p<0.05$ versus PU, +++ $p<0.005$ versus DEX (b) SEM fields of the surfaces after 1h incubation with whole blood. SEM were obtained at ×1000 (scale bar: 100 μm) and ×2000 (inset, scale bar: 10 μm) magnification.

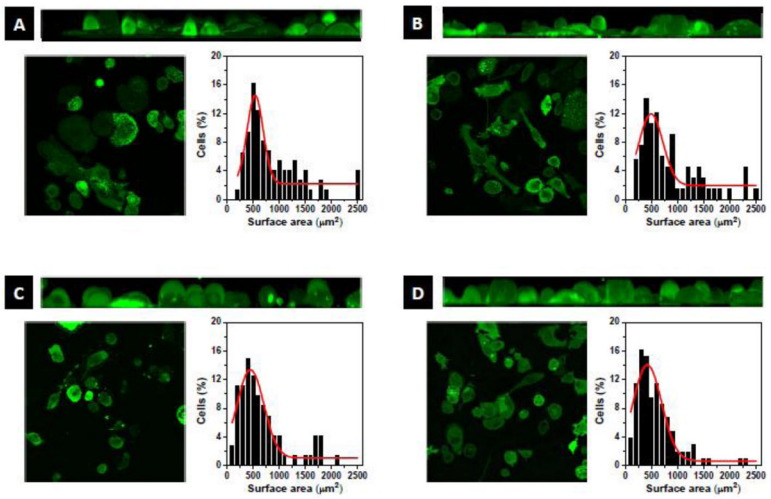


**Figure 2.**

Cell morphology. Morphology of PMA-stimulated THP-1 cells after 3 days exposure to (a) glass, (b) PU, (c) DEX and (d) DEX-Ag surfaces. Top: 3D-Volume view of XZ axis of the bottom left image series, Left: Single bottom slice of image series, Right: Cell surface area distribution.

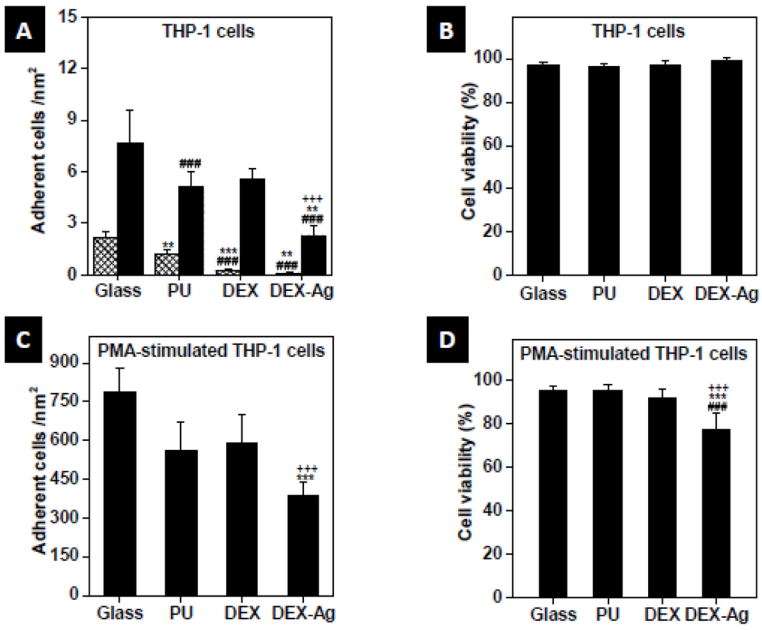


**Figure 3.**

Adhesion and cell viability. (a, c) Adhesion and (b, d) cell viability of after 1 day (grated bars) or 3 days (solid bars) exposure to glass, PU, DEX and DEX-Ag surfaces. Statistical significance: ### $p<0.005$ versus glass, *** $p<0.005$ versus PU, ** $p<0.05$ versus PU, +++ $p<0.005$ versus DEX.

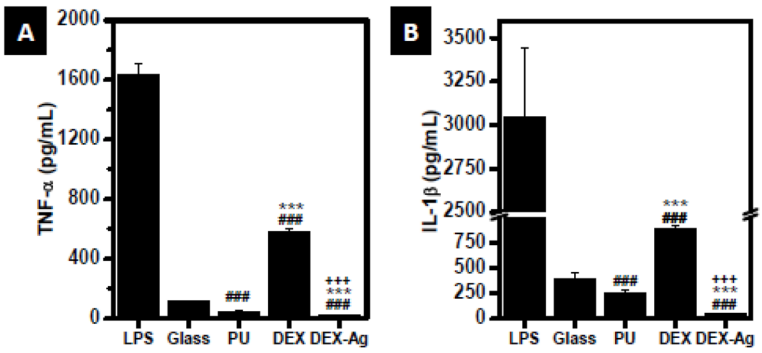


**Figure 4.**

Release of inflammatory cytokines. Amount of (a) TNF-α and (b) IL-1b released by PMA-stimulated THP-1 cells following incubation with glass, PU, DEX and DEX-Ag for 3 days, as determined by ELISA. LPS was used as a positive control. Statistical significance: ### $p<0.005$ versus glass, *** $p<0.05$ versus PU, +++ $p<0.005$ versus DEX.

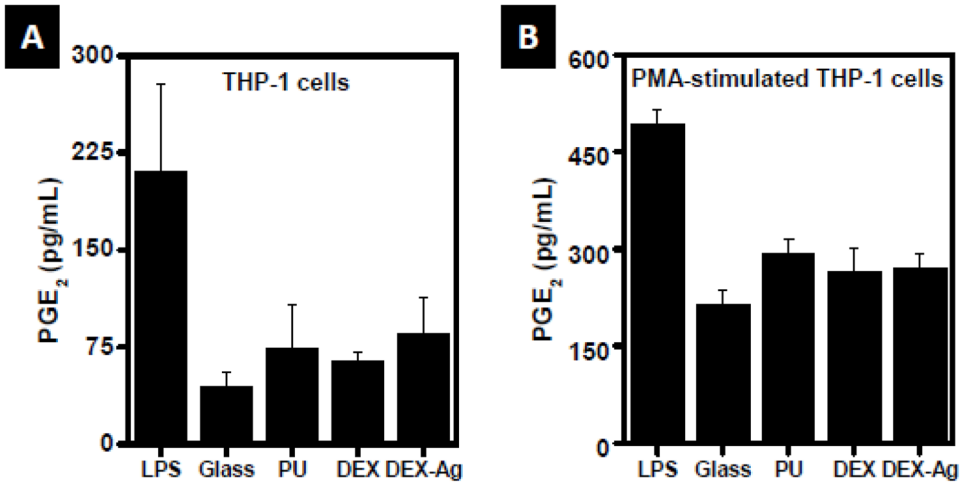


**Figure 5.**

Release of $PGE_2$. Amount released by (a) THP-1 cells and (b) PMA-stimulated THP-1 cells following incubation with glass, PU, DEX and DEX-Ag for 3 days, as determined by ELISA. LPS was used as a positive control. $PGE_2$ released is not statistically significant between surfaces ($p>0.05$).

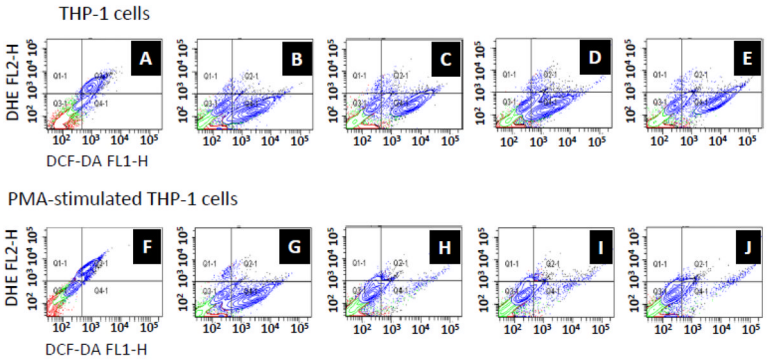


**Figure 6.**

ROS study. 2D-scatter plot showing superoxide (DHE) and hydrogen peroxide (DCF-DA) released following incubation with (c, h) PU, (d, i) DEX, (e, j) DEX-Ag as determined by flow cytometry. Cells incubated with (a, f) DCC and (b, g) $H_2O_2$ were used as a control for superoxide and hydrogen peroxide release, respectively.

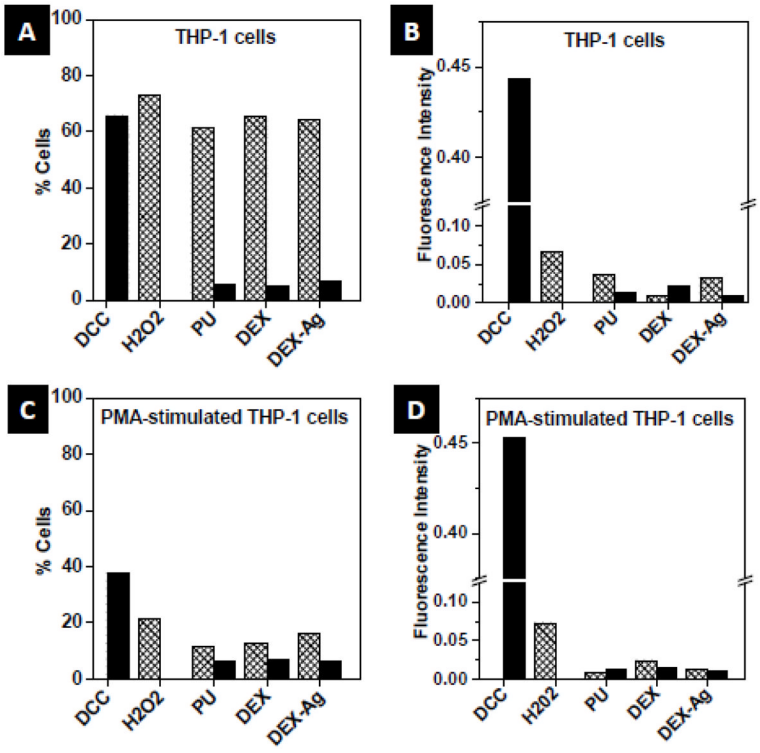


**Figure 7.**
ROS study. (a, c) Amount (%) and (b, d) fluorescence intensity of cells that released superoxide (solid bars) and hydrogen peroxide (grated bars) following incubation for 3 days with the surfaces or controls.

**Table 1**

Hemolytic activity of PU, DEX and DEX-Ag surfaces. Water and saline were used as positive and negative controls, respectively.

| Samples | Optical density at 545 nm | [Hb] (g/dL) | Hemolysis % |
|---|---|---|---|
| Water | 0.275 ± 0.026 | 0.16 ± 0.02 | 98.6 ± 9.2 |
| Saline | 0.00153 ± 0.00001 | 0.00089 ± 0.00001 | 0.537 ± 0.005 |
| PU | 0.00130 ± 0.00007 | 0.00075 ± 0.00039 | 0.455 ± 0.236 |
| DEX | 0.00147 ± 0.00005 | 0.00085 ± 0.00003 | 0.513 ± 0.019 |
| DEX-Ag | 0.00337 ± 0.00006 | 0.00190 ± 0.00003 | 1.180 ± 0.021 |